System investigation of a rolled-up metamaterial optical hyperlens structure

E. J. Smith, Z. Liu, Y. F. Mei, and O. G. Schmidt

Citation: Appl. Phys. Lett. **95**, 083104 (2009); doi: 10.1063/1.3211115
View online: https://doi.org/10.1063/1.3211115
View Table of Contents: http://aip.scitation.org/toc/apl/95/8
Published by the American Institute of Physics

System investigation of a rolled-up metamaterial optical hyperlens structure

E. J. Smith,[1,a)] Z. Liu,[2] Y. F. Mei,[1,a)] and O. G. Schmidt[1]
[1]*Institute for Integrative Nanosciences, IFW Dresden, Helmholtzstrasse. 20, D-01069 Dresden, Germany*
[2]*Department of Electrical and Computer Engineering, University of California, San Diego, 9500 Gilman Drive, La Jolla, California 92093, USA*

(Received 4 June 2009; accepted 30 July 2009; published online 24 August 2009)

An investigation of the material makeup and surrounding medium of an optical rolled-up hyperlens is presented. A working spectral range of the hyperlens for different material combinations is studied along with an examination of hyperlens immersion, which suppresses the diffraction of waves exiting the lens due to impedance matching, leading to a higher intensity output. This hyperlens immersion technique can be implemented into cell culture and molecular analysis. © *2009 American Institute of Physics*. [DOI: 10.1063/1.3211115]

Nanotechnology has led to exciting developments in science including the ability to manipulate material properties to create structures called metamaterials. Metamaterials open the door to creating negative index of refraction materials[1] and plasmonic materials which have lead to the development of such devices as the hyperlens[2–7] and to other devices for optoelectronic miniaturization and biological detection.[8] It has been noted that creating superlattices of different materials which are much smaller than the wavelength, leads to anisotropic materials that cannot be found naturally.[9] This has since been implemented into the idea of creating a lens, the hyperlens, which could image beyond the diffraction limit via transmission of high order evanescent waves in the near-field of an object[2–4] to propagating waves in the far-field, which can then be imaged using classical optics.

In this letter, we investigate the material combinations of a rolled-up layer system to optimize the hyperlensing effect. We begin with an investigation of different material make-ups, which allow for a low-loss and high transmission of the objects being magnified. We implement the well known effective media theory[9] and use a finite element method program COMSOL, to explore the material systems of rolled-up hyperlenses. We also examine the use of a hyperlens effectively as an immersion lens, by placing our rolled-up hyperlenses into a high index of refraction (n) liquid medium and impedance matching the lens to the surrounding medium. The diffraction which occurs at the outer surface of the lens can be lowered, allowing for a more efficient transmission into the far field. These studies are done in order to better classify the adequacies and deficiencies of different material combinations and surrounding medium for different sub-wavelength applications such as living cell and biomolecule analysis.

Our design is based on rolled-up nanotech[10] and has been proposed by our group to be used as a hyperlens.[11] More recently, even light transmission through a rolled-up layer system has been demonstrated.[12] By releasing a strained bilayer of metal and oxide, rolled-up metamaterials can be developed to be used for plasmonic devices including hyperlenses and metamaterial fiber optics.[13] This rolled-up, metal-oxide structure creates a circular superlattice geometry whose optical properties can be approximated using an effective media theory.[2–4,6] The effective media theory allows us to calculate the radial and tangential permittivity of the rolled-up structures in the following way: $\varepsilon_r=[(c_m+c_d)\varepsilon_m\varepsilon_d]/(\varepsilon_m+\varepsilon_d)$, and $\varepsilon_\theta=(\varepsilon_m+\varepsilon_d)/(c_m+c_d)$, where ε_m is the permittivity of the metal, ε_d is the permittivity of the dielectric, and c_m and c_d are the relative ratios of the metal and dielectric for a single bilayer [bottom Fig. 1(a)]. A rolled-up metal-oxide superlattice [Fig. 1(a)] leads to an anisotropic metamaterial whose permittivities can be approximated with the effective media theory [Fig. 1(b)], allowing

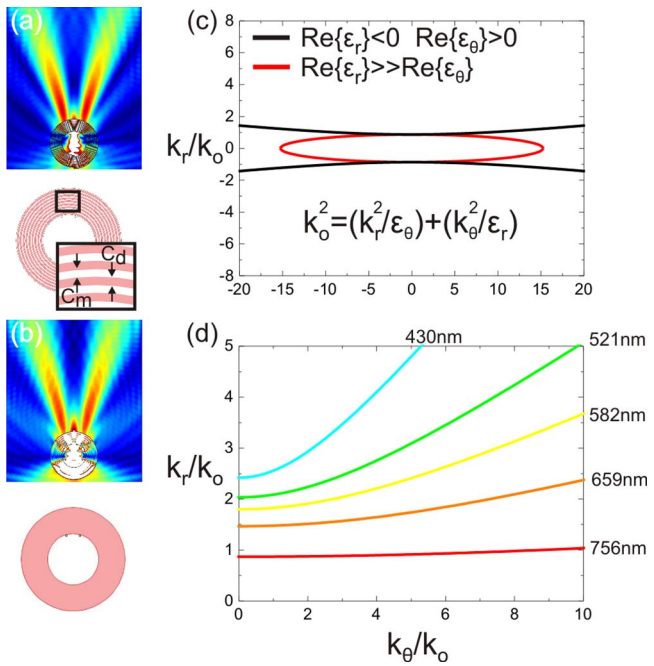

FIG. 1. (Color online) A diagram showing both a hyperlens using a realizable rolled-up TiO_2/Ag structure (a) and one using the effective permittivity theory (b). Objects being imaged are $\lambda/30$, separated by a distance of $\lambda/2$. (c) Using material combinations which result in anisotropy with characteristics of $\mathrm{Re}\{\varepsilon_r\}\gg\mathrm{Re}\{\varepsilon_\theta\}$, elliptical dispersion, or $\mathrm{Re}\{\varepsilon_r\}<0$ and $\mathrm{Re}\{\varepsilon_\theta\}>0$, hyperbolic dispersion, allow for the transmission of subwavelength information. (d) The dispersion relation curves for a TiO_2/Ag 5:1 ratio structure are plotted, showing a lens which is capable of working over the entire visible spectrum.

a)Authors to whom correspondence should be addressed. Electronic addresses: e.j.smith@ifw-dresden.de and y.mei@ifw-dresden.de.

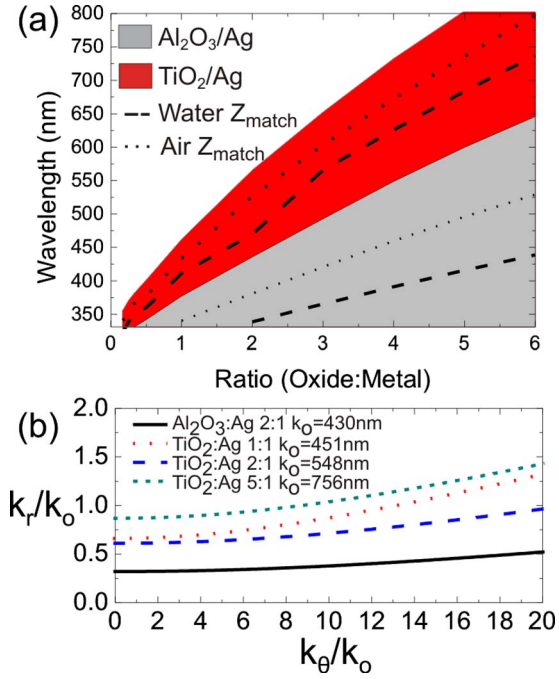

FIG. 2. (Color online) The tunable hyperbolic range of a hyperlens with different ratios of oxide to metal is presented. (a) The tunable hyperbolic range is defined to be where $\varepsilon_r<0$ and $\varepsilon_\theta>0$, given the criteria for the hyperlens effect (see Refs. 2–4 and 6). The dotted lines are the wavelengths required for impedance matching (Z_{match}) the given metamaterial lens with air, whereas the dashed are those required for matching with water which results in a high transmission into the far field. (b) The dispersion relation for different material makeups is shown for wavelengths near the plasma frequency of the lens, illustrating the fact that the dispersion relation approaches flatness which results in high resolution of high order wave vectors.

for a simplified geometry for simulation. Using the effective media theory and given the dispersion relation for transverse magnetic polarization, $k_o^2=(k_r^2/\varepsilon_\theta)+(k_\theta^2/\varepsilon_r)$ for this material, two possible anisotropies lead to the transmission of high order modes. The first is when $\mathrm{Re}\{\varepsilon_r\}<0$ and $\mathrm{Re}\{\varepsilon_\theta\}>0$, leading to a hyperbolic dispersion; the second is when $\mathrm{Re}\{\varepsilon_r\}\gg\mathrm{Re}\{\varepsilon_\theta\}$, leading to a highly elliptical dispersion [Fig. 1(c)]. Here, we focus on material combinations which result in hyperbolic dispersion relations. The k_θ governs the lowest size limit of an object and when the criteria of $\mathrm{Re}\{\varepsilon_r\}<0$ and $\mathrm{Re}\{\varepsilon_\theta\}>0$ is met, the dispersion relation becomes hyperbolic and k_θ becomes unbounded allowing for the transmission of subwavelength information.[2,3,6] As the hyperbolic function approaches flatness [shown in Fig. 1(d) for TiO_2:Ag 5:1], due to a larger anisotropy at different wavelengths, the resolution increases, resulting in the transmission of spatial information of arbitrary size into the far field. For a metamaterial consisting of TiO_2:Ag with a ratio of 5:1, the hyperbolic function is sufficiently flat for the entire visible spectral range.

Two important characteristics of optical magnification are resolution and transmission of the system. Taking a look at the hyperbolic working range of a metamaterial consisting of TiO_2/Ag and Al_2O_3/Ag (values of permittivities of oxides and metal taken from Refs. 14 and 15, respectively), a clear picture can be laid out of what material combination and wavelength can be used for optimal subdiffraction imaging, represented by the shaded regions of Fig. 2(a). The top boundary of the shaded regions are the plasmon frequency of the given metamaterial; lying directly below this line is where the hyperbolic dispersion relation approaches flatness, leading to the highest resolution. This graph shows that hyperlensing is obtainable over the entire visible range of light. The second important characteristic, transmission, can be optimized by addressing two points. The first is the loss arising in the lens, which can be calculated by examining $\mathrm{Im}\{\varepsilon_\theta\}$; due to the dispersion relation, this is the permittivity which influences the radial wave vector. In the two material systems investigated here, $\mathrm{Im}\{\varepsilon_\theta\}\ll 1$ as the wavelength approaches the plasma frequency of the material, leading to a negligible amount of loss over the distances we are interested in which are on the order of a few wavelengths. The loss arising in the metamaterial comes from the intrinsic loss of the metal and is unavoidable; however, the system can be optimized by increasing the filling ratio of the oxide and by shifting to a longer working wavelength which significantly decreases $\mathrm{Im}\{\varepsilon_\theta\}$ resulting in higher transmission. The second factor affecting transmission is impedance (Z) at the interface of the hyperlens and the surrounding medium.[5] An impedance mismatch at the interface leads to Fresnel reflection at the medium boundary, resulting in lower transmission. An impedance match can be achieved by working at a wavelength in which $\mathrm{sqrt}(\varepsilon_\theta)=n_{\mathrm{medium}}$, for a particular material makeup. The two dotted lines in Fig. 2(a) indicate the wavelength where this criterion is met for the particular metamaterials when working in a surrounding medium of air. The two dashed lines in Fig. 2(a) indicate the same criterion when working in a surrounding medium of water. Although the highest resolution obtainable and impedance matching of the system lie at different wavelengths, there is no big problem, since the dispersion relation is still relatively flat at these wavelengths. The dispersion relation for a few selected configurations is shown in Fig. 2(b) to illustrate the flatness of the relationship for different wavelengths and material configurations. Although for the impedance matched condition, the relation is not completely flat, the hyperlens still has the ability to resolve subwavelength objects. The importance of meeting the impedance matching condition is illustrated in Fig. 3 where using a hyperlens which is impedance matched with water, performs poorly in air [Fig. 3(a)], whereas in water [Fig. 3(b)] high resolution and transmission can be obtained. For this particular configuration, two objects emitting at 342 nm which are $\lambda/30$ (11.4 nm) in size, separated by $\lambda/2$ (171 nm), are magnified by a hyperlens which has an inner radius of λ (342 nm) and an outer radius of 3λ (1026 nm); resulting in a separation magnification power of 3 at the outer surface, coming from $M=r_{\mathrm{outer}}/r_{\mathrm{inner}}$.[3,4,6] However, due to the low loss system, the magnetic field is projected a significant distance from the outer surface and the magnification power can be increased if the imaging plane of the classical imaging system is moved away from the outer surface of the lens [as shown in Fig. 3(a) and 3(b)]. Figure 3(c) shows a magnification of $\sim$14 when the imaging plane is moved $\sim$3.5 μm from the outer surface of the hyperlens.

Using the hyperlens in practical experiments is the ultimate goal, and such area of interest is to study living subwavelength objects which are hard to resolve by other nanoimaging technology such as scanning electron microscopy or transmission electron microscopy, which require vacuum. Subwavelength studies of living cells and molecules could be realized using a hyperlens in the hyperbolic

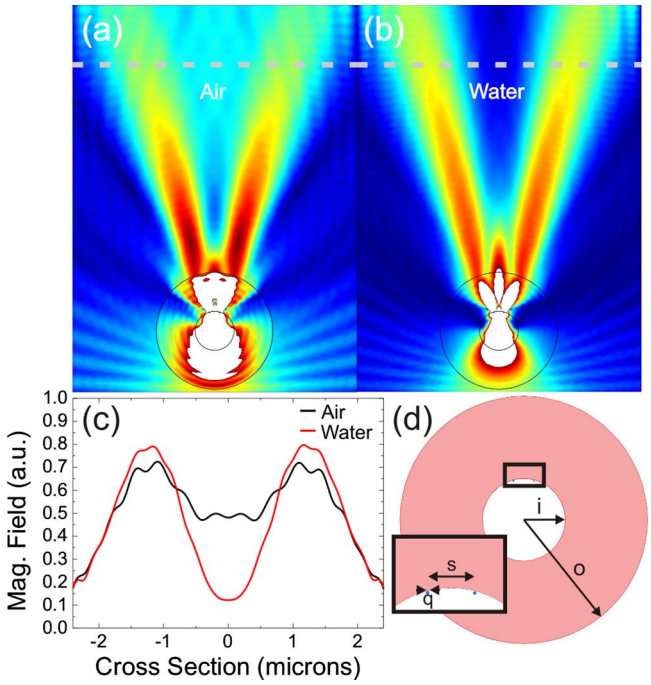

FIG. 3. (Color online) Impedance matching the lens to the surrounding medium becomes important for higher transmission and can give way to higher resolution than unmatched systems. This condition is met with $\mathrm{sqrt}(\varepsilon_\theta)=n_{\mathrm{medium}}$, and results in suppressed Fresnel reflection at the outer interface of the hyperlens for a higher output and better resolution. The normalized magnetic field distribution for (a) air and (b) water are shown. (c) A cross section of the magnetic field profile taken at 3.5 microns [dotted line in (a) and (b)] from the outer surface is shown to have higher resolution in water than in air. For this particular simulation, the effective permittivity is used for a 2:1 ratio of Al_2O_3:Ag at $\lambda=342$ nm leading to a $\mathrm{sqrt}(\varepsilon_\theta)=1.32$ and a index of refraction for water used was 1.33. (d) The geometry used is as follows; an inner diameter $i=\lambda$, outer diameter $o=3\lambda$, a separation of dots $s=\lambda/2$ and a dot size $q=\lambda/30$.

range shown in Fig. 1(c). Using a surrounding medium which allows for cell culture becomes an important step in realizing this goal. Studies have been done on a cell's ability to flourish in an environment with a substrate of Al_2O_3 and a surrounding medium of yeast-peptone-dextrose,[16] but were also found to survive in water, which is an optimal system for a rolled-up hyperlens. The introduction of water, or other liquids with higher index of refraction into the core of the lens can improve the resolution of the hyperlens whereas using the medium to surround the lens, the system can be impedance matched to allow for higher transmission. This effect is the same principle by which a classical immersion lens functions. Finding a material combination, Fig. 2(a), for the hyperlens and wavelength that yields $\mathrm{sqrt}(\varepsilon_\theta)=n_{\mathrm{medium}}$, we are able achieve an immersion hyperlens. As mentioned before, this effect can be seen when comparing a hyperlens in an air surrounding [Fig. 3(a)] to that of one in a water surrounding [Fig. 3(b)]. A look at the far-field profile [Fig. 3(c)] shows much better resolution in water than the same lens in air.

In this letter, we have described the effects in hyperlensing using different material makeups and surrounding medium in order to further classify the adequacies and deficiencies of a rolled-up hyperlens. We presented different material combinations which allow for hyperlensing over the entire visible range taking both resolution and transmission into account. By impedance matching the hyperlens to the surrounding medium, higher transmission is possible and results in an immersion hyperlens allowing for higher resolution of such a lens. This rolled-up immersion hyperlens could be used in live subwavelength cell-culture analysis which is presently not possible with other microscopy tools.

The authors would like to thank S. Kiravittaya and P. Cendula for fruitful discussions. This work is financially supported by the Volkswagen Foundation (1/84 072).

[1] V. G. Veselago, Sov. Phys. Usp. **10**, 509 (1968).
[2] B. Wood and J. B. Pendry, Phys. Rev. B **74**, 115116 (2006).
[3] A. Salandrino and N. Engheta, Phys. Rev. B **74**, 075103 (2006).
[4] Z. Jacob, L. V. Aleksezev, and E. E. Narimanov, Opt. Express **14**, 8247 (2006).
[5] A. V. Kildishev and E. E. Narimanov, Opt. Lett. **32**, 3432 (2007).
[6] H. Lee, Z. Liu, Y. Xiong, C. Sun, and X. Zhang, Opt. Express **15**, 15886 (2007).
[7] Z. Liu, H. Lee, Y. Xiong, C. Sun, and X. Zhang, Science **315**, 1686 (2007).
[8] W. L. Barnes, A. Dereux, and T. W. Ebbesen, Nature (London) **424**, 824 (2003).
[9] S. M. Rytov, Sov. Phys. JETP **29**, 605 (1955).
[10] O. G. Schmidt and K. Eberl, Nature (London) **410**, 168 (2001).
[11] Y. F. Mei, G. S. Huang, A. A. Solovev, E. Bermúdez Ureña, I. Mönch, F. Ding, T. Reindl, R. K. Y. Fu, P. K. Chu, and O. G. Schmidt, Adv. Mater. **20**, 4085 (2008).
[12] S. Schwaiger, M. Bröll, A. Krohn, A. Stemmann, C. Heyn, Y. Stark, D. Stickler, D. Heitmann, and S. Mendach, Phys. Rev. Lett. **102**, 163903 (2009).
[13] E. J. Smith, Z. Liu, Y. F. Mei, and O. G. Schmidt, Nano Lett. (to be published), DOI: 10.1021/nl900550j.
[14] E. D. Palik, *Handbook of Optical Constants of Solids* (Academic, San Diego, CA, 1998).
[15] P. B. Johnson and R. W. Christy, Phys. Rev. B **6**, 4370 (1972).
[16] G. S. Huang, Y. F. Mei, D. J. Thurmer, E. Coric, and O. G. Schmidt, Lab Chip **9**, 263 (2009).